Effects of the spin–orbit interaction on the spin polarization of quantum dots in the presence of Andreev reflection

2008 J. Phys.: Condens. Matter 20 195220

(http://iopscience.iop.org/0953-8984/20/19/195220)

J. Phys.: Condens. Matter **20** (2008) 195220 (7pp) doi:10.1088/0953-8984/20/19/195220

Effects of the spin–orbit interaction on the spin polarization of quantum dots in the presence of Andreev reflection

Hui Pan[1] **and Rong Lü**[2]

[1] Department of Physics, Beijing University of Aeronautics and Astronautics, Beijing 100083, People's Republic of China
[2] Center for Advanced Study, Tsinghua University, Beijing 100084, People's Republic of China

Received 20 February 2008, in final form 25 March 2008
Published 17 April 2008
Online at stacks.iop.org/JPhysCM/20/195220

Abstract
The effects of the spin–orbit interaction on the spin polarization of quantum dots in an Aharonov–Bohm interferometer in the presence of Andreev reflection are investigated theoretically. The spin polarization of quantum dots appears on the resonance of Andreev reflection, which depends sensitively on the spin-dependent phase difference caused by the spin–orbit interaction. The amplitude and the sign of the spin polarization in the two quantum dots can be controlled by the gate voltage, the bias and the magnetic flux. Furthermore, by tuning the magnetic flux the spin polarizations in the two quantum dots can even have opposite signs from each other. This provides an efficient mechanism for controlling the amplitude and sign of the spin polarization in the two quantum dots.

1. Introduction

Much experimental and theoretical research has been devoted to how to efficiently control and manipulate the spin in the quantum dot (QD), since it is an important and challenging issue in semiconductor spintronics [1, 2]. Some of the schemes that have been proposed to polarize and manipulate the spin in the QD include coupling the QD to ferromagnetic leads [3, 4] or using an external magnetic field to polarize the spin of the QD [5]. However, it is difficult to inject the spin from a ferromagnetic lead into a semiconductor QD or to confine a very strong magnetic field to a small region of the QD. To avoid these difficulties, some theoretical studies based on the spin–orbit (SO) interaction have been proposed to realize the spin-polarized current or the spin accumulation [6–9]. SO interaction can couple the spin and the orbital motion of an electron, thereby giving a useful handle for manipulating and controlling the electron spin by external electric fields. The spin precession phenomenon induced by the SO interaction has been proposed for the realization of a spin transistor [10]. The phase difference $\Delta\varphi_R = 2\alpha_R m^* L/\hbar^2$ of the spin precession between the source and drain contact is a function of the Rashba spin–orbit coupling strength α, the electron effective mass m^* and the separation L between the source and drain electrode [10–12]. In experiments the Rashba spin–orbit coupling strength can be tuned by an external electric field or gate voltage [13–16]. The effects of the SO interaction on the transport phenomena in an Aharonov–Bohm (AB) interferometer containing one QD result in an interesting spin-dependent phase coherence phenomenon, in which spin-up and spin-down electrons travelling through the upper and lower arms can acquire different phases [9].

Recently, an AB interferometer containing two QDs has been realized, in which quantum phase coherence is detectable by interference experiments [17–19]. The open parallel double quantum dot (DQD) threaded by a magnetic flux makes the quantum transport phenomena rich and varied, in which the electron retains coherence. Inspired by these recent experiments in parallel DQDs, several theoretical works have been done on Fano resonance in the parallel DQD system with and without the interdot coupling [20–22]. As a controllable two-level system, the parallel DQD system therefore becomes a promising candidates for a quantum qubit in quantum computation based on solid-state devices [23]. A qubit is the basic unit in the achievement of quantum computing. Among many quantum two-level systems, the spin of a QD is an ideal candidate for such a purpose. One of the challenges in exploiting the spin of a QD as a qubit is to efficiently control its local spin polarization. On the other hand, superconductor coupled mesoscopic hybrid systems have

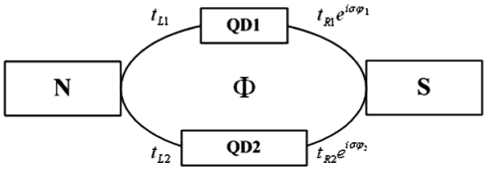

Figure 1. Schematic diagram of a parallel double quantum dot (DQD) system connected with (left) a normal-metal (N) lead and (right) a superconducting (S) lead. The Rashba SO interaction is assumed to exist only inside the QD1 and QD2, which results in two spin-dependent phases, φ_1 and φ_2.

become an interesting field in recent years because of both their fundamental physics and potential applications in future nanoelectronics [24–27]. The Andreev reflection happens at the normal-metal/superconductor (N/S) interface [28], in which an incoming electron from the normal side is reflected as a hole and a Cooper pair is transferred into the superconducting condensate. More recently, a superconducting quantum interference device with two QDs embedded in its arms has been realized [29, 30], where no coupling exists between the two parallel QDs. One may expect that the interplay of the spin property of the Andreev reflection process and the SO interaction in the QD will add new physics to mesoscopic hybrid systems, and to the future applications of spintronics.

Motivated by this, we investigate the spin polarization in the N/DQD/S system. The device with the two QDs can be regarded as an AB interferometer threaded by magnetic fluxes [29, 30]. The scheme of the system is plotted in figure 1. Two QDs are embedded into opposite arms of the AB ring. We assume that the Rashba SO interaction exists only inside the QD and the leads are free from this interaction. The Rashba SO interaction effect would induce a spin precession of the electrons tunnelling through the ith QD with a spin-dependent phase shift $\sigma\varphi_i$. By using the nonequilibrium Green's function (NGF) technique [31–34], we have analysed the SO interaction effects on the spin polarization in the N/DQD/S system. Some novel resonant features have been found. The spin polarization in the QD caused by the SO interaction appears on the resonant Andreev reflection, whose magnitude and direction can be easily controlled by the gate voltage and the bias. The direction of the spin polarization can also be tuned by the magnetic flux, which provides another way to control the spin polarization of each quantum dot. The rest of this paper is organized as follows. In section 2 we present the model Hamiltonian and derive the formula of the electron occupation number and the spin polarization in the QD by using the NGF technique. In section 3 we study the effects of the SO interaction on the electron occupation number. Control of the spin polarization with the system parameters such as the gate voltage, the bias and the magnetic flux are discussed in detail. Finally, a brief summary is given in section 4.

2. Physical model and formula

The N/DQD/S system under consideration is modelled by the following Hamiltonian:

$$H = H_{\rm L} + H_{\rm R} + H_{\rm D} + H_{\rm T}. \tag{1}$$

$H_{\rm L}$ describes noninteracting electrons in the left normal-metal lead

$$H_{\rm L} = \sum_{k\sigma} \epsilon_k a^\dagger_{k\sigma} a_{k\sigma}, \tag{2}$$

where $a^\dagger_{\alpha,k\sigma}$ ($a_{\alpha,k\sigma}$) are the creation (annihilation) operators of the electron in the left lead. $H_{\rm R}$ is the standard BCS Hamiltonian for the right superconducting lead

$$H_{\rm R} = \sum_{p\sigma} \epsilon_p b^\dagger_{p\sigma} b_{p\sigma} + \sum_p [\Delta b^\dagger_{p\uparrow} b^\dagger_{-p\downarrow} + {\rm H.c.}], \tag{3}$$

where Δ is the energy gap. The chemical potential of the right superconducting lead is set as $\mu_{\rm R} = 0$ due to gauge invariance. The chemical potential of the left normal-metal lead is $\mu_{\rm L} = eV$ with V the bias. $H_{\rm D}$ models the parallel double quantum dots

$$H_{\rm D} = \sum_{\sigma,i=1,2} (\varepsilon_{i\sigma} - eV_{{\rm g}i}) d^\dagger_{i\sigma} d_{i\sigma}, \tag{4}$$

where $d^\dagger_{i\sigma}$ ($d_{i\sigma}$) represents the creation (annihilation) operator of the electron in the ith QD ($i = 1, 2$) with spin $\sigma = \uparrow/\downarrow$. The spin-degenerate energy level $\varepsilon_{i\sigma}$ is measured relative to the Fermi energy defined by the right lead, which can be tuned by the gate voltage $V_{{\rm g}i}$. $H_{\rm T}$ represents the tunnelling coupling between the double quantum dots and leads

$$H_{\rm T} = \sum_{k\sigma,i=1,2} (t_{{\rm L}i} {\rm e}^{{\rm i}\phi_{{\rm L}i}} a^\dagger_{k\sigma} d_{i\sigma} + {\rm H.c.}) + \sum_{p\sigma,i=1,2} (t_{{\rm R}i} {\rm e}^{{\rm i}\phi_{{\rm R}i} + i\sigma\varphi_i} b^\dagger_{p\sigma} d_{i\sigma} + {\rm H.c.}). \tag{5}$$

In the model presented, the Rashba SO interaction only exists inside the two QDs, which gives rise to spin precession [10–12]. The second-quantized form of the Rashba SO interaction can cause two effects [9]: (1) an extra spin-dependent phase factor in the hopping matrix element between the leads and the QD; (2) an interlevel spin-flip term. Since the ith QD considered here only contains one single energy level, $\varepsilon_{i\sigma}$, the Rashba SO interaction inside the ith QD gives rise to an extra spin-dependent phase factor. The phase $\varphi_i = -\alpha_{{\rm R}i} m^* L_i/\hbar^2$ also describes the spin precession angle, with $\alpha_{{\rm R}i}$ and L_i being the Rashba SO interaction strength and the size of the ith QD [10–12]. When an electron tunnels through the QD, the spin-dependent extra phase is generated in the path, and thus $t_{{\rm R}i}$ changes into $t_{{\rm R}i}{\rm e}^{{\rm i}\sigma\varphi_i}$ [9]. The phase difference $\varphi = \varphi_2 - \varphi_1$ plays an important role in the spin polarization in the QDs. For simplicity, the electron–electron interaction is neglected here. Since the Coulomb interaction prevents the tunnelling of Cooper pairs into the quantum dot, electrons in each pair tunnel one by one via virtual processes, resulting in suppression of the Andreev tunnelling [32, 35, 36]. Therefore, it is expected that the Coulomb interaction can decrease the spin polarization in the Coulomb blockade regime. $\phi_{\alpha i}$ is the phase shift of the electron tunnelling from the ith QD to the αth lead with $\phi_{\rm L1} = -\phi_{\rm L2} = -\phi_{\rm R1} = \phi_{\rm R2} = -\phi/4$ and $\phi = 2\pi\Phi/\phi_0$, where Φ is the total magnetic flux threading into the AB ring in the flux quantum unit $\phi_0 = hc/e$.

Because of the right superconductor lead, it is convenient to use the 4×4 Nambu representation to include the physics of Andreev reflection. The tunnelling matrices of the hopping elements in the present Nambu representation are

$$\mathbf{t}_{\mathrm{L}\sigma} = \begin{pmatrix} t_{\mathrm{L}1}\mathrm{e}^{-\mathrm{i}\phi/4} & 0 & 0 & 0 \\ 0 & -t_{\mathrm{L}1}^{*}\mathrm{e}^{\mathrm{i}\phi/4} & 0 & 0 \\ 0 & 0 & t_{\mathrm{L}2}\mathrm{e}^{\mathrm{i}\phi/4} & 0 \\ 0 & 0 & 0 & -t_{\mathrm{L}2}^{*}\mathrm{e}^{-\mathrm{i}\phi/4} \end{pmatrix}, \quad (6)$$

and

$$\mathbf{t}_{\mathrm{R}\sigma} = \begin{pmatrix} t_{\mathrm{R}1}\mathrm{e}^{\mathrm{i}\phi/4+\mathrm{i}\sigma\varphi_1} & 0 & 0 & 0 \\ 0 & -t_{\mathrm{R}1}^{*}\mathrm{e}^{-\mathrm{i}\phi/4-\mathrm{i}\sigma\varphi_1} & 0 & 0 \\ 0 & 0 & t_{\mathrm{R}2}\mathrm{e}^{-\mathrm{i}\phi/4+\mathrm{i}\sigma\varphi_2} & 0 \\ 0 & 0 & 0 & -t_{\mathrm{R}2}^{*}\mathrm{e}^{\mathrm{i}\phi/4-\mathrm{i}\sigma\varphi_2} \end{pmatrix}, \quad (7)$$

respectively. Although only $\mathbf{t}_{\mathrm{R}\sigma}$ really depend on spin, we add a spin subscript for the tunnel matrix $\mathbf{t}_{\mathrm{L}\sigma}$ for consistency. In the Nambu representation, each hopping element of the tunnelling matrix has its only meaning [33, 34]: $\mathbf{t}_{\mathrm{L}/R\sigma 11}$ ($\mathbf{t}_{\mathrm{L}/R\sigma 22}$) for an electron (hole) with spin σ ($-\sigma$) tunnelling between the L/R lead and the QD 1, and $\mathbf{t}_{\mathrm{L}/R\sigma 33}$ ($\mathbf{t}_{\mathrm{L}/R\sigma 44}$) for an electron (hole) with spin σ ($-\sigma$) tunnelling between the L/R lead and the QD 2.

The electron occupation number in the two QDs can be calculated from standard NGF techniques. The retarded and lesser Green's function are defined as $\mathbf{G}_{\sigma}^{\mathrm{r}}(t,t') = -\mathrm{i}\theta(t-t')\langle\{\Psi_{\sigma}(t), \Psi_{\sigma}^{\dagger}(t')\}\rangle$ and $\mathbf{G}_{\sigma}^{<}(t,t') = \mathrm{i}\langle\Psi_{\sigma}^{\dagger}(t')\Psi_{\sigma}(t)\rangle$, respectively, with the operator $\Psi_{\sigma} = (d_{1\sigma}^{\dagger}, d_{1\bar{\sigma}}, d_{2\sigma}^{\dagger}, d_{2\bar{\sigma}})^{\dagger}$. Let $\mathbf{g}_{\sigma}^{\mathrm{r}}(\epsilon)$ and $\mathbf{G}_{\sigma}^{\mathrm{r}}(\epsilon)$ denote the Fourier-transformed retarded Green's function of the QD without and with the coupling to the leads. By using the Dyson equation, the retarded Green function of the system can be obtained as $\mathbf{G}_{\sigma}^{\mathrm{r}}(\epsilon) = [\mathbf{g}_{\sigma}^{\mathrm{r}}(\epsilon)^{-1} - \mathbf{\Sigma}_{\sigma}^{\mathrm{r}}(\epsilon)]^{-1}$, where $\mathbf{\Sigma}_{\sigma}^{\mathrm{r}} = \mathbf{\Sigma}_{\mathrm{L}\sigma}^{\mathrm{r}} + \mathbf{\Sigma}_{\mathrm{R}\sigma}^{\mathrm{r}}$. The lesser Green function of the system can be obtained by using the Keldysh equation $\mathbf{G}_{\sigma}^{<}(\epsilon) = \mathbf{G}_{\sigma}^{\mathrm{r}}(\epsilon)\mathbf{\Sigma}_{\sigma}^{<}(\epsilon)\mathbf{G}_{\sigma}^{\mathrm{a}}(\epsilon)$, where $\mathbf{G}_{\sigma}^{\mathrm{a}} = (\mathbf{G}_{\sigma}^{\mathrm{r}})^{\dagger}$ and $\mathbf{\Sigma}_{\sigma}^{<} = \mathbf{\Sigma}_{\mathrm{L}\sigma}^{<} + \mathbf{\Sigma}_{\mathrm{R}\sigma}^{<}$. In the Nambu representation, $\mathbf{g}_{\sigma}^{\mathrm{r}}(\epsilon)$ can be written as

$$\mathbf{g}_{\sigma}^{\mathrm{r}}(\epsilon) = \begin{pmatrix} \frac{1}{\epsilon-\varepsilon_{1\sigma}+\mathrm{i}0^{+}} & 0 & 0 & 0 \\ 0 & \frac{1}{\epsilon+\varepsilon_{1\bar{\sigma}}+\mathrm{i}0^{+}} & 0 & 0 \\ 0 & 0 & \frac{1}{\epsilon-\varepsilon_{2\sigma}+\mathrm{i}0^{+}} & 0 \\ 0 & 0 & 0 & \frac{1}{\epsilon+\varepsilon_{2\bar{\sigma}}+\mathrm{i}0^{+}} \end{pmatrix}, \quad (8)$$

where $\bar{\sigma}$ labels the opposite spin direction to σ. The retarded self-energy under the wide-bandwidth approximation can be derived from the definition [33]

$$\mathbf{\Sigma}_{\mathrm{L}\sigma}^{\mathrm{r}}(\epsilon) = \sum_{k} \mathbf{t}_{\mathrm{L}\sigma}^{*}\mathbf{g}_{k}^{\mathrm{r}}(\epsilon)\mathbf{t}_{\mathrm{L}\sigma} = -\frac{\mathrm{i}}{2}\mathbf{\Gamma}_{\mathrm{L}\sigma}$$
$$= -\frac{\mathrm{i}}{2}\begin{pmatrix} \Gamma_{1}^{\mathrm{L}} & 0 & \Gamma_{12}^{\mathrm{L}}\mathrm{e}^{\mathrm{i}\phi/2} & 0 \\ 0 & \Gamma_{1}^{\mathrm{L}} & 0 & \Gamma_{12}^{\mathrm{L}}\mathrm{e}^{-\mathrm{i}\phi/2} \\ \Gamma_{12}^{\mathrm{L}}\mathrm{e}^{-\mathrm{i}\phi/2} & 0 & \Gamma_{2}^{\mathrm{L}} & 0 \\ 0 & \Gamma_{12}^{\mathrm{L}}\mathrm{e}^{\mathrm{i}\phi/2} & 0 & \Gamma_{2}^{\mathrm{L}} \end{pmatrix}, \quad (9)$$

and

$$\mathbf{\Sigma}_{\mathrm{R}\sigma}^{\mathrm{r}}(\epsilon) = \sum_{k} \mathbf{t}_{\mathrm{R}\sigma}^{*}\mathbf{g}_{p}^{\mathrm{r}}(\epsilon)\mathbf{t}_{\mathrm{R}\sigma} = -\frac{\mathrm{i}}{2}\rho_{\mathrm{R}}(\epsilon)$$
$$\times \begin{pmatrix} \Gamma_{1}^{\mathrm{R}} & -\Gamma_{1}^{\mathrm{R}}\mathrm{e}^{-\mathrm{i}\phi/2-2\mathrm{i}\sigma\varphi_1}\frac{\Delta}{\epsilon} & \Gamma_{12}^{\mathrm{R}}\mathrm{e}^{-\mathrm{i}\phi/2-\mathrm{i}\sigma(\varphi_1-\varphi_2)} & -\Gamma_{12}^{\mathrm{R}}\mathrm{e}^{-\mathrm{i}\sigma(\varphi_1+\varphi_2)}\frac{\Delta}{\epsilon} \\ -\Gamma_{1}^{\mathrm{R}}\mathrm{e}^{\mathrm{i}\phi/2+2\mathrm{i}\sigma\varphi_1}\frac{\Delta}{\epsilon} & \Gamma_{1}^{\mathrm{R}} & -\Gamma_{12}^{\mathrm{R}}\mathrm{e}^{-\mathrm{i}\sigma(\varphi_1+\varphi_2)}\frac{\Delta}{\epsilon} & \Gamma_{12}^{\mathrm{R}}\mathrm{e}^{-\mathrm{i}\phi/2-\mathrm{i}\sigma(\varphi_1-\varphi_2)} \\ \Gamma_{12}^{\mathrm{R}}\mathrm{e}^{\mathrm{i}\phi/2+\mathrm{i}\sigma(\varphi_1-\varphi_2)} & -\Gamma_{12}^{\mathrm{R}}\mathrm{e}^{-\mathrm{i}\sigma(\varphi_1+\varphi_2)}\frac{\Delta}{\epsilon} & \Gamma_{2}^{\mathrm{R}} & -\Gamma_{2}^{\mathrm{R}}\mathrm{e}^{-\mathrm{i}\phi/2-2\mathrm{i}\sigma\varphi_2}\frac{\Delta}{\epsilon} \\ -\Gamma_{12}^{\mathrm{R}}\mathrm{e}^{\mathrm{i}\sigma(\varphi_1+\varphi_2)}\frac{\Delta}{\epsilon} & \Gamma_{12}^{\mathrm{R}}\mathrm{e}^{\mathrm{i}\phi/2+\mathrm{i}\sigma(\varphi_1-\varphi_2)} & -\Gamma_{12}^{\mathrm{R}}\mathrm{e}^{-\mathrm{i}\phi/2+2\mathrm{i}\sigma\varphi_2}\frac{\Delta}{\epsilon} & \Gamma_{2}^{\mathrm{R}} \end{pmatrix}, \quad (10)$$

where $\mathbf{g}_{k}^{\mathrm{r},<}(\epsilon)$ and $\mathbf{g}_{p}^{\mathrm{r},<}(\epsilon)$ are the Green's functions of the electron in the isolated left and right leads, respectively. The factor $\rho_{\mathrm{R}}(\epsilon)$ in the right self-energy is defined as [32]

$$\rho_{\mathrm{R}}(\epsilon) = \begin{cases} \dfrac{|\epsilon|}{\sqrt{(\epsilon^2-\Delta^2)}} & |\epsilon| > \Delta \\ \dfrac{\epsilon}{\mathrm{i}\sqrt{(\Delta^2-\epsilon^2)}} & |\epsilon| < \Delta. \end{cases} \quad (11)$$

The linewidth functions describing the coupling between the DQD and the leads are defined as $\Gamma_{ij}^{\alpha} = 2\pi t_{\alpha i}^{*}t_{\alpha j}\rho_{\alpha}^{N}$ with ρ_{α}^{N} being the density states of the α lead in a normal-metal state. Thus $\Gamma_{12}^{\mathrm{L}} = \sqrt{\Gamma_{1}^{\mathrm{L}}\Gamma_{2}^{\mathrm{L}}}$ and $\Gamma_{12}^{\mathrm{R}} = \sqrt{\Gamma_{1}^{\mathrm{R}}\Gamma_{2}^{\mathrm{R}}}$. Under the wide-bandwidth approximation, the linewidth functions are independent of the energy variable. Similarly, the lesser self-energies are derived from the definition [33]

$$\mathbf{\Sigma}_{\mathrm{L}\sigma}^{<}(\epsilon) = \sum_{k} \mathbf{t}_{\mathrm{L}\sigma}^{*}\mathbf{g}_{k}^{<}(\epsilon)\mathbf{t}_{\mathrm{L}\sigma} = \mathrm{i}\mathbf{f}_{\mathrm{L}}(\epsilon)\mathbf{\Gamma}_{\mathrm{L}\sigma}$$
$$= \mathrm{i}\begin{pmatrix} f_{\mathrm{L}}(\epsilon-eV) & 0 & 0 & 0 \\ 0 & f_{\mathrm{L}}(\epsilon+eV) & 0 & 0 \\ 0 & 0 & f_{\mathrm{L}}(\epsilon-eV) & 0 \\ 0 & 0 & 0 & f_{\mathrm{L}}(\epsilon+eV) \end{pmatrix}\mathbf{\Gamma}_{\mathrm{L}\sigma}, \quad (12)$$

and

$$\mathbf{\Sigma}_{\mathrm{R}\sigma}^{<}(\epsilon) = \sum_{k} \mathbf{t}_{\mathrm{R}\sigma}^{*}\mathbf{g}_{p}^{<}(\epsilon)\mathbf{t}_{\mathrm{R}\sigma} = \mathrm{i}\mathbf{f}_{\mathrm{R}}(\epsilon)\tilde{\rho}_{\mathrm{R}}(\epsilon)$$
$$\times \begin{pmatrix} \Gamma_{1}^{\mathrm{R}} & -\Gamma_{1}^{\mathrm{R}}\mathrm{e}^{-\mathrm{i}\phi/2-2\mathrm{i}\sigma\varphi_1}\frac{\Delta}{\epsilon} & \Gamma_{12}^{\mathrm{R}}\mathrm{e}^{-\mathrm{i}\phi/2-\mathrm{i}\sigma(\varphi_1-\varphi_2)} & -\Gamma_{12}^{\mathrm{R}}\mathrm{e}^{-\mathrm{i}\sigma(\varphi_1+\varphi_2)}\frac{\Delta}{\epsilon} \\ -\Gamma_{1}^{\mathrm{R}}\mathrm{e}^{\mathrm{i}\phi/2+2\mathrm{i}\sigma\varphi_1}\frac{\Delta}{\epsilon} & \Gamma_{1}^{\mathrm{R}} & -\Gamma_{12}^{\mathrm{R}}\mathrm{e}^{-\mathrm{i}\sigma(\varphi_1+\varphi_2)}\frac{\Delta}{\epsilon} & \Gamma_{12}^{\mathrm{R}}\mathrm{e}^{-\mathrm{i}\phi/2-\mathrm{i}\sigma(\varphi_1-\varphi_2)} \\ \Gamma_{12}^{\mathrm{R}}\mathrm{e}^{\mathrm{i}\phi/2+\mathrm{i}\sigma(\varphi_1-\varphi_2)} & -\Gamma_{12}^{\mathrm{R}}\mathrm{e}^{-\mathrm{i}\sigma(\varphi_1+\varphi_2)}\frac{\Delta}{\epsilon} & \Gamma_{2}^{\mathrm{R}} & -\Gamma_{2}^{\mathrm{R}}\mathrm{e}^{\mathrm{i}\phi/2-2\mathrm{i}\sigma\varphi_2}\frac{\Delta}{\epsilon} \\ -\Gamma_{12}^{\mathrm{R}}\mathrm{e}^{\mathrm{i}\sigma(\varphi_1+\varphi_2)}\frac{\Delta}{\epsilon} & \Gamma_{12}^{\mathrm{R}}\mathrm{e}^{\mathrm{i}\phi/2+\mathrm{i}\sigma(\varphi_1-\varphi_2)} & -\Gamma_{12}^{\mathrm{R}}\mathrm{e}^{-\mathrm{i}\phi/2+2\mathrm{i}\sigma\varphi_2}\frac{\Delta}{\epsilon} & \Gamma_{2}^{\mathrm{R}} \end{pmatrix}, \quad (13)$$

where the Fermi distribution matrices $\mathbf{f}_{\mathrm{L}}$ and $\mathbf{f}_{\mathrm{R}}$ only have the diagonal components as $f_{\mathrm{L}ii} = f(\epsilon + (-1)^{i}eV)$ and

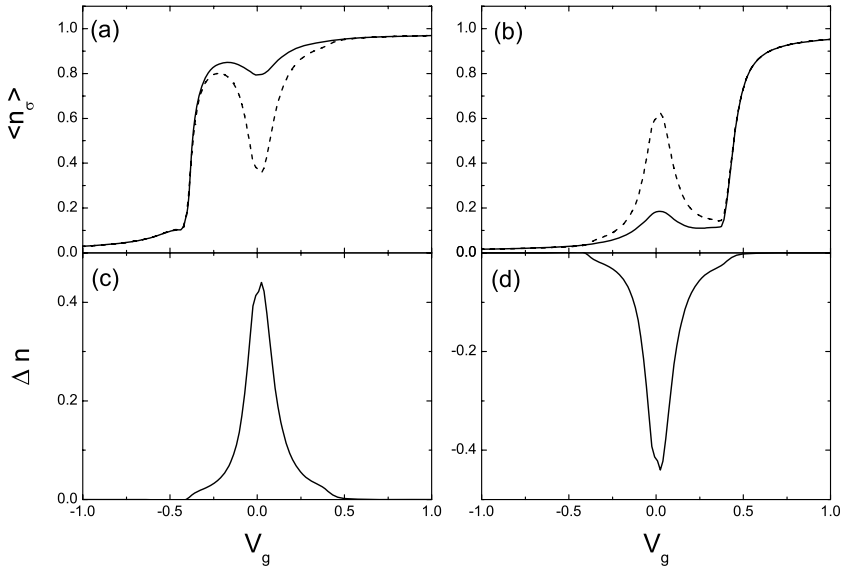

Figure 2. The occupation number $\langle n_\sigma \rangle$ versus the gate voltage V_g for spin-up (solid line) and spin-down (dashed line) electrons at the bias (a) $V = 0.4$ and (b) $V = -0.4$, respectively. (c), (d) The corresponding spin polarization Δn. Other parameters are $\varepsilon_1 = -\varepsilon_2 = 0.05$, $\varphi = 0.25\pi$, $\phi = 0$, and $\Gamma_1^L = \Gamma_2^L = \Gamma_1^R = \Gamma_2^R = 0.1$.

$f_{Rii} = f(\epsilon)$ with $i = 1 \ldots 4$, respectively. $\tilde{\rho}_R(\epsilon)$ is the corresponding dimensionless BCS density of states $\tilde{\rho}_R(\epsilon) = \theta(|\epsilon| - \Delta)|\epsilon|/\sqrt{\epsilon^2 - \Delta^2}$. The expectation values of the electron occupation number $n_{i\sigma} = d_{i\sigma}^\dagger d_{i\sigma}$ are give by

$$\langle n_{1\sigma} \rangle = -i \int \frac{d\epsilon}{2\pi} G^<_{\sigma,11}, \tag{14}$$

and

$$\langle n_{2\sigma} \rangle = -i \int \frac{d\epsilon}{2\pi} G^<_{\sigma,33}. \tag{15}$$

The spin polarization is defined as

$$\Delta n_{1(2)} = \langle n_{1(2)\uparrow} \rangle - \langle n_{1(2)\downarrow} \rangle. \tag{16}$$

In the following, we focus on the case of $eV < \Delta$ and perform the calculations at zero temperature in units of $\hbar = e = 1$. The energy gap of the superconductor is fixed as $\Delta = 1$. All the energy quantities in the calculations are scaled by Δ.

3. Results and discussions

To clarify the physics of how the spin-dependent phase φ influences the transport properties, a qualitative analysis of the effective spin-dependent tunnelling strength can be given before the detailed numerical calculations. Consider an electron tunnelling to the left lead from QD 2: it has two paths. One path is through direct tunnelling. The other is to first travel to the right lead and then tunnel to the left lead through QD 1. For simplicity, the tunnelling probability through QD 1 is assumed to be T_{D1}, and only the first order tunnelling process is considered. Then, the total effective tunnelling strength $T_{L\sigma}$ between QD 2 and the left lead is $T_{L\sigma} = |t_{L2} + t_{L1}T_{D1}t_{1R}(-i\pi\rho)t_{R2}|^2 = |t_{L2}|^2 + |\pi\rho t_{L1}T_{D1}t_{1R}t_{R2}|^2 + 2\pi\rho|t_{L2}t_{L1}T_{D1}t_{1R}t_{R2}|\sin(\sigma\varphi + \phi)$. This means that the tunnelling strength heavily depends on the spin σ due to the spin–orbit interaction within the QDs. For example, $T_{L\uparrow} > T_{L\downarrow}$ when $\varphi = 0.25\pi$ and $\phi = 0$, while $T_{L\uparrow} < T_{L\downarrow}$ when $\varphi = 0.25\pi$ and $\phi = \pi$.

The spin polarization can happen on the resonant Andreev reflection due to the different tunnelling strengths for spin-up and spin-down electrons. We first study the case in which the two QD levels are very close, where the spin polarization for the two QDs is almost the same at the same gate voltage. The occupation number $n_\sigma (= n_{1\sigma} \simeq n_{2\sigma})$ and the corresponding spin polarization $\Delta n (= \Delta n_1 \simeq \Delta n_2)$ versus the gate voltage V_g are plotted in figure 2, corresponding to the bias $V = 0.4$ and $V = -0.4$, respectively. The spin-dependent phase is set as $\varphi = 0.25\pi$, and the two QD energy levels are set as $\varepsilon_1 = -\varepsilon_2 = 0.05$. There is a step from 0 to 1 in the curves when the dot level sweeps the chemical potential μ_L by tuning the gate voltage, which indicates an electron filling to the QD. Since there is no single-particle state in the superconducting gap, electron filling to the QD is mainly determined by the left normal-metal lead, resulting in a step linked to μ_L. When the dot level lines up with μ_R, resonant Andreev reflection may occur. One Andreev dip or peak is superposed on the step-like curve for $V = 0.4$ or -0.4, respectively. Furthermore, $n_\uparrow$ and $n_\downarrow$ are separated dramatically on the Andreev reflection resonances at the dip or peak. The spin polarization of the QD is caused by the nonzero spin-dependent phase φ, since the effective tunnelling strength for spin-up electrons $T_{L\uparrow}$ is larger than that for spin-down electrons $T_{L\downarrow}$. For the case of $V > 0$, a Cooper pair is formed by a spin-up and a spin-down electron in the process of Andreev reflection. Since it is easier for the spin-up electrons to tunnel from the left lead into the QDs than for the spin-down electrons, the spin-down electrons will be depleted by the spin-up electrons in the process of Andreev reflection, resulting in a spin polarization $\Delta n > 0$ in the QDs. While for the case of $V < 0$, a Cooper pair is converted into a spin-up and a spin-down electron in the QD. Since it

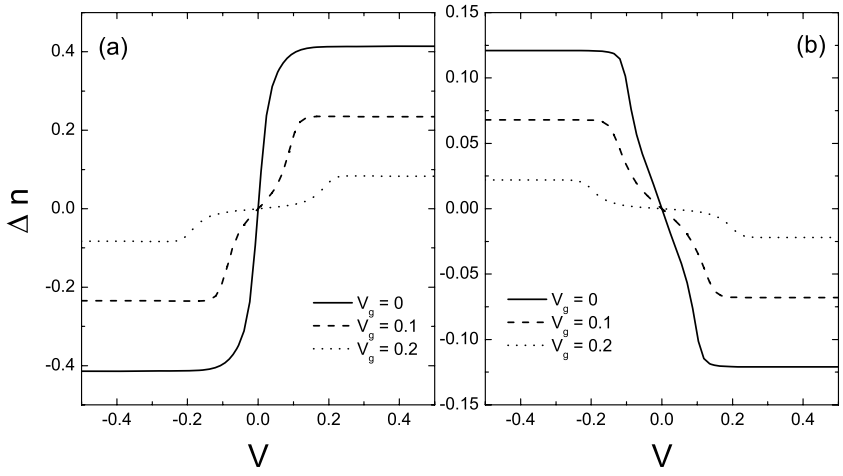

Figure 3. The spin polarization Δn versus the bias V for (a) $\phi = 0$ and (b) $\phi = \pi$ at different gate voltages $V_g = 0$ (solid line), $V_g = 0.1$ (dashed line) and $V_g = 0.2$ (dotted line). Other parameters are the same as those in figure 1.

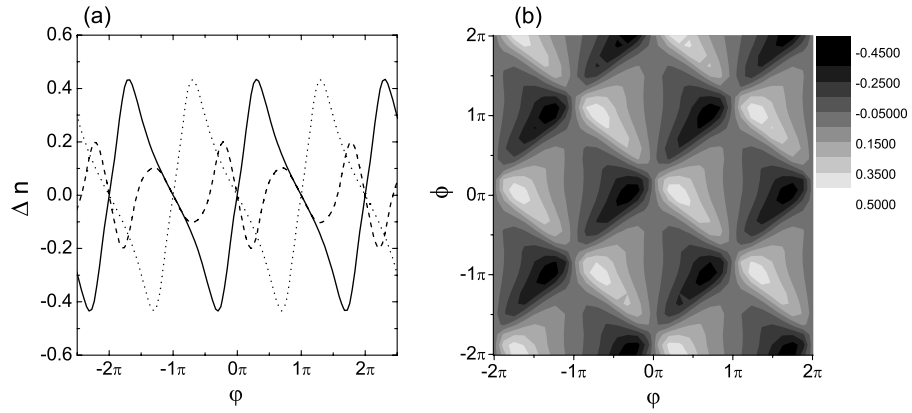

Figure 4. (a) The spin polarization Δn versus the phase φ at different magnetic fluxes $\phi = 0$ (solid line), $\phi = 0.5\pi$ (dashed line) and $\phi = \pi$ (dotted line). (b) The images of Δn as a function of φ and ϕ. Other parameters are the same as those in figure 1.

is much easier for spin-up electrons than spin-down electrons to escape to the empty states of left lead, a reversed negative spin polarization $\Delta n < 0$ appears.

The strength and the direction of the spin polarization can be easily controlled and manipulated by varying the bias voltage V, as shown in figure 3. It is worth mentioning that the nonzero spin-dependent phase φ caused by the SO interaction is necessary in the present system. It is seen that the spin polarization Δn is zero at $V = 0$, while the nonzero Δn emerges under a finite bias. The amplitude of the spin polarization increases rapidly with increasing V from 0 and finally reaches a constant. If the bias is decreased from 0, the spin polarization changes its sign and its direction is reversed. This means that the direction of spin polarization can be easily controlled by changing the external bias. The reason for the reversal of the spin polarization is related to the Andreev reflection processes at positive or negative bias. When there exists a magnetic flux of $\phi = \pi$, the spin polarization can also be reversed. The reason is that the magnetic flux changes the tunnelling strength for spin-up and spin-down electrons as mentioned above, which results in the reverse of the spin polarization. It is also shown that Δn decreases with increasing V_g, since the Andreev reflection is suppressed when the resonant level is moved away from the Fermi energy by tuning the gate voltage.

Figure 4 presents the dependence of Δn on the phase φ for different magnetic fluxes ϕ. Δn versus φ exhibits a periodic function with the period of 2π. For $\varphi = 2n\pi$ with n the integer, there is no spin polarization. Furthermore, the magnetic flux can change not only the magnitude but also the sign of Δn as mentioned above. It is seen that the sign of Δn for $\phi = 0$ is just exchanged with that for $\phi = \pi$. The spin-dependent phase φ and the magnetic phase ϕ together can lead a complex picture for Δn. The images of the Δn versus the φ and ϕ are also plotted. The bright regions correspond to positive Δn and the dark regions to negative Δn.

Next, we study the case that the difference between the two QD levels is large enough that two QDs have quite different spin polarizations at the same gate voltage. The dependence of the spin polarization Δn_i for the ith QD on the gate voltage V_g are plotted in figure 5(a). The bias voltage is set as $V = 0.4$ and the dot energy levels are set as $\varepsilon_1 = \varepsilon_2 = -0.2$. In the curves, two resonant peaks emerge whose positions are at $V_g = 0, 0.2$ for Δn_1 and at $V_g = -0.2, 0$ for

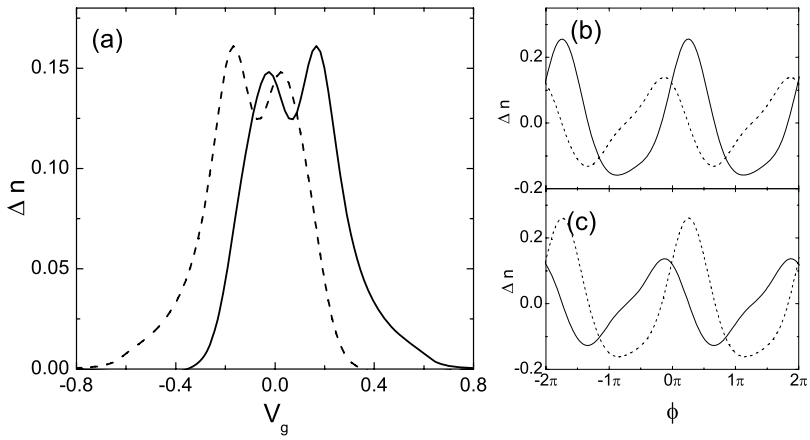

Figure 5. The spin polarization Δn_1 (solid line) and Δn_2 (dashed line) for $V = 0.4$ versus (a) V_g at $\phi = 0$, and versus ϕ at (b) $V_g = 0.1$ and (c) $V_g = -0.1$, respectively. Other parameters are $\varepsilon_1 = -\varepsilon_2 = 0.2$, $\varphi = 0.25\pi$ and $\Gamma_1^L = \Gamma_2^L = 0.1$ and $\Gamma_1^R = \Gamma_2^R = 0.2$.

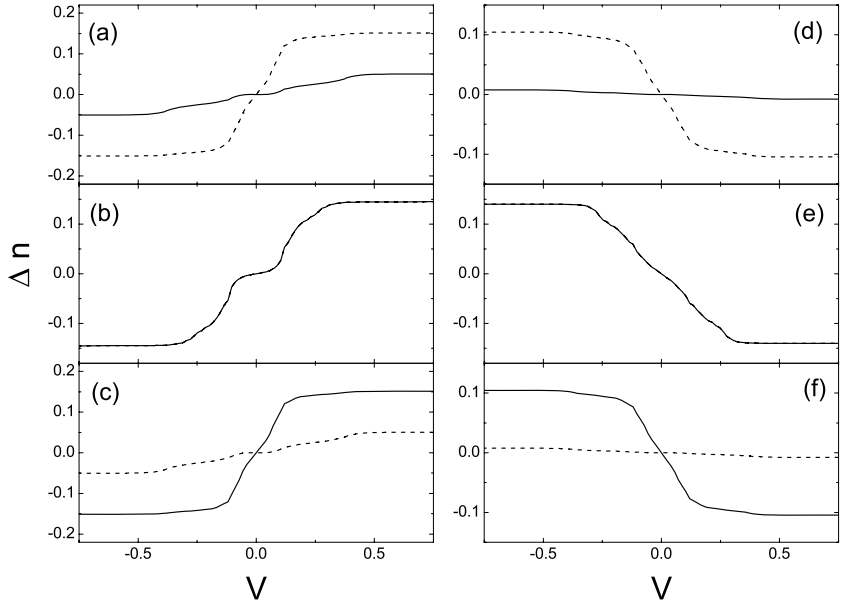

Figure 6. The spin polarization Δn_1 (solid line) and Δn_2 (dashed line) versus V for $\phi = 0$ at (a) $V_g = -0.2$, (b) $V_g = 0$ and (c) $V_g = 0.2$. (d)–(f) show the corresponding information for $\phi = \pi$. Other parameters are the same as those in figure 5.

Δn_2, respectively. When ε_1 (ε_2) lines up with μ_R at $V_g = -0.2$ ($V_g = 0.2$), resonant Andreev reflection may occur in which a spin-up and a spin-down electron in QD can leak into the superconductor lead by forming a Cooper pair. For a certain gate voltage $V_g = 0$, the two resonant states ε_1 and ε_2 are symmetrical about μ_R and are both below μ_L, which can also lead to the resonant Andreev reflection. An electron incident with appropriate energy can tunnel from the lead into the QD state ε_1 (ε_2), and then can be Andreev reflected as a hole back to the QD state ε_2 (ε_1). With increasing V_g, QD 2 first has greater spin polarization than QD 1, and then QD 1 and QD 2 have the same spin polarization, and finally QD 1 has greater spin polarization than QD 2. Figures 5(b) and (c) present the dependence of the Δn_1 and Δn_2 on the magnetic flux ϕ at $V_g = 0.1$ and -0.1, respectively. It is noted that Δn_1 and Δn_2 are just exchanged by changing V_g from 0.1 to -0.1. What is more interesting is that Δn_1 and Δn_2 can be different not only in magnitude but also in sign within some certain ranges of magnetic flux. For example (see figure 5(b)), $\Delta n_1 > 0$ but $\Delta n_2 < 0$ near $\phi = 0.5\pi$, $n_{1\uparrow} \simeq n_{2\downarrow}$ near $\phi = 0$, and $\Delta n_1 > \Delta n_2 > 0$ near $\phi = 0.1\pi$, respectively. This provides an efficient way to control the spin polarization of each QD by tuning the magnetic flux and the gate voltage.

As mentioned above, the direction of the spin polarization is dependent on the bias and the magnetic flux. Figure 6 shows that the signs of Δn_1 and Δn_2 are both controllable by V and ϕ. When there is no magnetic flux at $\phi = 0$, the signs of Δn_1 and Δn_2 are positive for $V > 0$ and negative for $V < 0$, respectively. Two cases are considered in the following: (1) only QD 1 or QD 2 is strongly spin polarized at $V_g = 0.2$ or $V_g = -0.2$, respectively; (2) both QD 1 and QD 2 are strongly spin polarized at $V_g = 0$. It is seen that Δn_2 (Δn_1) is much larger than Δn_1 (Δn_2) at $V_g = -0.2$ ($V_g = 0.2$), while they are almost the same at $V_g = 0$. For the first case of $V_g = -0.2$

($V_g = 0.2$), Δn_1 (Δn_2) is near zero and changes little with increasing V from 0, while Δn_2 (Δn_1) changes greatly and finally reaches a constant at $V = \varepsilon_2 - V_g$ ($V = |\varepsilon_1 - V_g|$). With decreasing V from 0, Δn_1 (Δn_2) is still near zero, while Δn_2 (Δn_1) changes its sign from positive to negative and also reaches a large negative value. For the second case of $V_g = 0$, $\Delta n_1 \simeq \Delta n_2$, and their signs can also be reversed by changing the bias V from positive to negative. However, when there exists a nonzero magnetic flux of $\phi = \pi$, the spin polarizations of QD 1 and QD 2 are reversed compared with those of $\phi = 0$. The signs of Δn_1 and Δn_2 become negative for $V > 0$ and positive for $V < 0$. This provides another way to tune the direction of the spin polarization of the two quantum dots by varying the magnetic flux.

Finally, some discussions are given about the realizability of the device shown in figure 1. A parallel DQD system with a size within the phase coherence length has already been fabricated in experiments by using a two-dimensional electron gas, which can be coupled to normal-metal [17, 18] or superconductor electrodes [29, 30]. Since the spin polarization is caused by the phase difference between the two QDs, one can assume that only one QD contains the Rashba SO interaction in order to make the system more controllable and favourable in experiments. Furthermore, since the Rashba SO interaction strength can be tuned in experiments by an external electric field or gate voltage [13–16], the assumption of adjusting the spin-dependent phase shift is reasonable.

4. Summary

In summary, the effects of the spin–orbit interaction on the spin polarization of two QDs embedded in an Aharonov–Bohm interferometer connected with one normal-metal lead and one superconductor lead are investigated theoretically by using the nonequilibrium Green's function methods. Due to the nonzero spin-dependent phase difference between the two quantum dots caused by the spin–orbital interaction, the spin polarization of the quantum dots appears on the Andreev reflection resonance. The magnitude and the sign of the spin polarization can be controlled by the system parameters such as the gate voltage V_g, the bias V and the magnetic flux ϕ threading the AB interferometer, respectively. The sign of the spin polarization is positive for $V > 0$ and negative for $V < 0$, when the magnetic flux is $\phi = 0$. However, the sign of the spin polarization becomes negative for $V > 0$ and positive for $V < 0$, when the magnetic flux becomes $\phi = \pi$. By controlling V_g, spin polarization can exist in one or both of the two QDs. Furthermore, the spin polarizations in the two QDs can even have opposite directions by tuning ϕ. This provides an efficient mechanism to control the amplitude and sign of the spin polarization in the two quantum dots, which may have practical applications for future spintronics.

Acknowledgments

HP would like to acknowledge Professor T H Lin for many helpful discussions. This project is supported by the National Natural Science Foundation of China (grant no. 10704005) and the Beijing Municipal Science and Technology Commission (grant no. 2007B017). RL was supported by the MOE of China (grant no. 200221) and the Ministry of Science and Technology of China (grant no. 2006CB605105).

References

[1] Zutic I, Fabian J and Das Sarma S 2004 *Rev. Mod. Phys.* **76** 323
[2] Wolf S A, Awschalom D D, Buhrman R A, Daughton J M, Molnar S V, Roukes M L, Chtchelkanova A Y and Treger D M 2001 *Science* **294** 1488
[3] Recher P, Sukhorukov E V and Loss D 2000 *Phys. Rev. Lett.* **85** 1962
[4] Zhu Y, Lin T H and Sun Q F 2004 *Phys. Rev.* B **69** 121302(R)
[5] Imamoglu A, Awschalom D D, Burkard G, DiVincenzo D P, Loss D, Sherwin M and Small A 1999 *Phys. Rev. Lett.* **83** 4204
[6] Ionicioiu R and D'Amico I 2003 *Phys. Rev.* B **67** 041307(R)
[7] Frustaglia D and Richter K 2004 *Phys. Rev.* B **69** 235310
Frustaglia D, Hentschel M and Richter K 2001 *Phys. Rev. Lett.* **87** 256602
[8] Koga T, Nitta J, Takayanagi H and Datta S 2002 *Phys. Rev. Lett.* **88** 126601
[9] Sun Q F, Wang J and Guo H 2005 *Phys. Rev.* B **71** 165310
[10] Datta S and Das B 1990 *Appl. Phys. Lett.* **56** 665
[11] Mireles F and Kirczenow G 2001 *Phys. Rev.* B **64** 024426
[12] Matsuyama T, Hu C M, Grundler D, Meier G and Merkt U 2002 *Phys. Rev.* B **65** 155322
[13] Nitta J, Akasaki T, Takayanagi H and Enoki T 1997 *Phys. Rev. Lett.* **78** 1335
[14] Heida J P, van Wees B J, Kuipers J J, Klapwijk T M and Borghs G 1998 *Phys. Rev.* B **57** 11911
[15] Grundler D 2000 *Phys. Rev. Lett.* **84** 6074
[16] Matsuyama T, Kursten R, Messner C and Merkt U 2000 *Phys. Rev.* B **61** 15588
[17] Holleitner A W, Decker C R, Qin H, Eberl K and Blick R H 2001 *Phys. Rev. Lett.* **87** 256802
[18] Holleitner A W, Blick R H, Hüttel A K, Eberl K and Kotthaus J P 2002 *Science* **297** 70
[19] Chen J C, Chang A M and Melloch M R 2004 *Phys. Rev. Lett.* **92** 176801
[20] Konig J and Gefen Y 2002 *Phys. Rev.* B **65** 045316
Kubala B and Konig J 2002 *Phys. Rev.* B **65** 245301
[21] Ladron de Guevara M L, Claro F and Orellana P A 2003 *Phys. Rev.* B **67** 195335
[22] Lopez R, Sanchez D, Lee M, Choi M S, Simon P and Le Hur K 2005 *Phys. Rev.* B **71** 115312
[23] Loss D and DiVincenzo D P 1998 *Phys. Rev.* A **57** 120
[24] Knorr N, Schneider M A, Diekhoner L, Wahl P and Kern K 2002 *Phys. Rev. Lett.* **88** 096804
[25] Buitelaar M R, Nussbaumer T and Schönenberger C 2002 *Phys. Rev. Lett.* **89** 256801
[26] Wei Y, Wang J, Guo H, Mehrez H and Roland C 2001 *Phys. Rev.* B **63** 195412
[27] Bena C, Vishveshwara S, Balents L and Fisher M P A 2002 *Phys. Rev. Lett.* **89** 037901
[28] Beenakker W J 1997 *Rev. Mod. Phys.* **69** 731
[29] Jarillo-Herrero P, van Dam J A and Kouwenhoven L P 2006 *Nature* **439** 953
[30] Cleuziou J P, Wernsdorfer W, Bouchiat V, Ondarcuhu T and Monthioux M 2006 *Nat. Nanotechnol.* **1** 53
[31] Jauho A P, Wingreen N S and Meir Y 1994 *Phys. Rev.* B **50** 5528
[32] Yeyati A L, Cuevas J C, Lopez-Davalos A and Martin-Rodero A 1997 *Phys. Rev.* B **55** R6137
[33] Sun Q F, Wang J and Lin T H 1999 *Phys. Rev.* B **59** 13126
[34] Pan H and Lin T H 2006 *Phys. Rev.* B **74** 235312
[35] Kang K 1998 *Phys. Rev.* B **58** 9641
[36] Fazio R and Raimondi R 1998 *Phys. Rev. Lett.* **80** 2913